Non-seasonal variations of atmospheric CO2 concentrations at Amsterdam Island

A. Gaudry, P. Monfray, G. Polian, G. Bonsang, B. Ardouin, A. Jegou, G. Lambert

Tellus (1991), *43B*, 136–143

Non-seasonal variations of atmospheric CO_2 concentrations at Amsterdam Island

By A. GAUDRY*, P. MONFRAY, G. POLIAN*, G. BONSANG, B. ARDOUIN, A. JEGOU* and G. LAMBERT, *Centre des Faibles Radioactivités, Laboratoire mixte CNRS/CEA, Avenue de la Terrasse, F-91198 Gif-sur-Yvette Cedex, France*

(Manuscript received 19 March 1990; in final form 3 October 1990)

ABSTRACT

The atmospheric CO_2 monitoring at Amsterdam island has shown a general increasing trend of the increase rate, which shifted from 1.1 ppm year^{-1} in January 1981 to 1.8 ppm year^{-1} in January 1989. Besides this general trend, three different kinds of variations were observed: (a) seasonal variations, whose magnitude is small at this station, that is less than ± 0.7 ppm; (b) small non-seasonal variations, as in 1985, likely related to changes in the atmospheric transport, also observed in other stations, but with different magnitudes and features; (c) important non-seasonal variations of the order of 1 ppm, negatively correlated to ENSO events of 1983 and 1987, with delays of 6 and 3 to 4 months, respectively. These variations are ascribed to a general change of the CO_2 emissions to the atmosphere, resulting from global climatic perturbations, rather than to transport processes. This is particularly shown at our sampling site through ^{222}Rn monitoring, that enables us to characterize direct air injections from South Africa into subantarctic areas.

1. Introduction

The present increase of atmospheric CO_2 could be ascribed to fossil fuel combustion, whose annual flux represents about twice this increase rate (Rotty, 1987). However, the history of CO_2 concentrations may challenge this statement, as important variations have also been observed in ice cores, long before any industrial activity (Barnola et al., 1987). Further, significant changes in fuel consumption do not appear to correlate with similar variations on the CO_2 increase rate. Moreover, since the beginning of the Mauna Loa records, some changes in the increase rate of the atmospheric CO_2 concentration have been related to changes in the sea surface temperature (SST) of the Pacific Ocean (Newell and Weare, 1977; Bacastow, 1979; Machta et al., 1977; Elliott and Angell, 1987). More particularly, Komhyr et al., (1985) found that El Niño Southern Oscillation events (ENSO) of 1972, 1976, and 1982–1983 were associated with slower-than-normal atmospheric CO_2 increase during the first year, followed by very rapid CO_2 increase in the following year.

In a previous paper, Ascensio-Parvy et al. (1984) observed similar relations at Amsterdam Island from data obtained during 1980–1983. Their results were confirmed by Gaudry et al. (1987), who found a correlation between the Sea Surface Temperature (SST) anomaly in the Pacific Ocean in 1982–1983 due to the El Niño event and calculated a release of about 6-billion tons CO_2 into the atmosphere. Elliott and Angell (1987) and Keeling et al. (1989) also studied the relations between ENSO events and the CO_2 increase rate. The occurrence of another ENSO event in 1987 offers a new opportunity to compare the CO_2 increase rate (dCO_2/dt), with ENSO manifestations. With this aim, CO_2 monitoring at Amsterdam Island is particularly interesting, owing to the smallness of both the local interference and the seasonal variations which allows the use of simplified statistical treatment.

* Also at ORSTOM/TAAF-Paris, France.

2. Site and methods

The site and method were described by Gaudry et al. (1983). The station (37°47'S; 77°31'E), 5000 km off South Africa, is part of the Background Air Pollution Monitoring Network (BAPMoN) of the World Meteorological Organization (WMO). The sampling point is located at the NNW of the island, on the edge of a 55 m high cliff, at an elevation of 9 m from the soil.

Typically marine air masses are carried by the following wind conditions: 260° < direction < 300° and velocities > 8 m s^{-1}, and 300° < direction < 360° and 0° < direction < 040° with velocities > 4 m s^{-1}. These severe criteria cancel southerly winds, which are frequent, but the corresponding air masses cross the island northwards, and are influenced by the local vegetation.

2.1. *Atmospheric CO_2 measurements*

A non-dispersive infrared analyzer URAS 2T was used during the whole period. The air was dried by means of a cryogenical water trap. The temperature of the cool bath was recorded daily, enabling for further corrections when residual water remained due to eventual temperatures warmer than −55°C. In normal field conditions, the reproducibility achieved is ±0.05 ppm. Each minute, the wind speed and direction values, as well as the atmospheric CO_2 concentration, were gathered on floppy disks. Subsequently, hourly mean values were determined for every parameter. By selecting data corresponding to marine air masses, complying with the wind conditions already mentioned, we obtain a first background data set.

2.2. *Scale*

Standard gases used from October 1980 to 1985 were CO_2 mixtures in N_2, certified by the Scripps Institution of Oceanography (SIO). The effect of the carrier gas was determined by CO_2 mixtures in synthetic air, and was intercompared with the 1985 WMO Scale in air. It is worth noting that 4 mixtures in synthetic air, accurately prepared by a gravimetrical method, had concentrations agreeing within 0.17 ppm with the SIO scale. Since 1986, this scale was compared twice a year with another accurate gravimetrical scale made of 6 CO_2 mixtures in synthetic air. Both scales are still being used at Amsterdam island. No significant drift was observed between these scales during the study period.

3. CO_2 long-term trend

The monthly mean values of CO_2: ($y(t)$), calculated from selected data are shown in Table 1 and Fig. 1. This figure displays a clear increase, with short-term fluctuations. As a 1st step, the long term trend can be simulated by a 4th degree polynomial:

$$\mathrm{P4}(t) = \sum_{n=0}^{n=4} a_n t^n,$$

which minimizes the deviation $y(t) - \mathrm{P4}(t)$. The corresponding coefficients (a_n) of P4(t) appear in Table 2. The origin of the time, in months, is arbitrary, being $t = 1$ for January 1980. From P4(t), we can determine a mean increase rate of about 1.5 ppm $year^{-1}$ between January 1981 and January 1989. However, during this period, the increase rate increased from about 1.1 ppm $year^{-1}$ in January 1981 to about 1.8 ppm $year^{-1}$ in January 1989.

The residual difference ($r(t) = y(t) - \mathrm{P4}(t)$) is shown in Fig. 2. These values vary with a bimodal periodicity corresponding to a seasonal effect, with 2 maxima, in winter and summer respectively, and whose magnitudes are rather variable, but not exceeding ±0.7 ppm. Moreover, a smoothed curve of $r(t)$, called $L(t)$, obtained by a 12-month running mean, displays non-seasonal variations.

The derivative of the function $\mathrm{P4}(t) + L(t)$ gives every month the average increase rates of atmospheric CO_2. In Fig. 3, this function has been

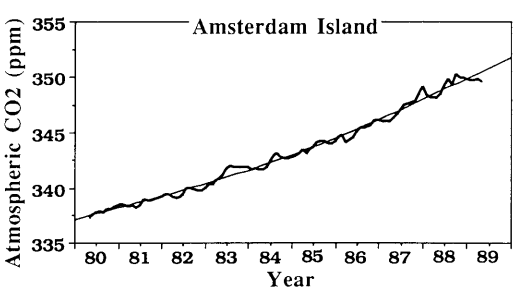

Fig. 1. Monthly mean concentrations of atmospheric CO_2.

Table 1. *Monthly mean atmospheric CO_2 concentrations calculated for all values of ^{222}Rn (left), or when $^{222}Rn < 1$ pCi m^{-3} (right), and monthly mean ^{222}Rn concentration selected by marine sector; values in brackets are simulated*

Year	Month	CO_2(ppm) all Radon	CO_2(ppm) Rn < 1 pCi/m3	Rn (marine sect.)	Year	Month	CO_2(ppm) all Radon	CO_2(ppm) Rn < 1 pCi/m3	Rn (marine sect.)
1980	5	337.29	337.55	1.53	1984	11	342.6	342.63	0.61
	6	337.49	337.44	1.96		12	342.6	342.15	0.68
	7	337.65	337.72	1.91	1985	1	(342.7)		0.71
	8	337.76	337.77	0.92		2	(342.9)		0.82
	9	337.75	337.65	0.66		3	(343.1)		0.99
	10	338	337.82	0.69		4	343.4	343.38	1.20
	11	338	338.08	1.18		5	343.1	343.11	1.28
	12	338.3	338.00	0.67		6	343.4	343.27	1.44
1981	1	338.4	338.35	0.70		7	343.7	343.63	1.49
	2	338.5	338.43	0.77		8	344.1	344.14	1.60
	3	338.4	338.29	0.68		9	344.2	344.19	1.63
	4	338.3	338.27	0.62		10	344.2	344.21	0.91
	5	338.4	338.47	0.87		11	344	344.01	0.66
	6	338.2	338.15	1.12		12	344	344.15	0.66
	7	338.4	338.34	1.37	1986	1	344.2	344.22	0.58
	8	338.9	338.78	1.20		2	344.6	344.6	0.94
	9	338.8	338.62	1.30		3	344.8	344.82	0.85
	10	338.8	338.84	1.12		4	344.1	344.12	0.76
	11	338.9	338.92	0.60		5	344.3	344.33	1.89
	12	339.1	339.06	0.58		6	344.6	344.59	1.32
1982	1	339.2	339.23	0.52		7	345.1	345.05	1.43
	2	339.4	339.66	0.50		8	345.5	345.46	0.92
	3	339.4	339.41	0.63		9	345.5	345.51	1.19
	4	339.2	339.15	0.94		10	345.6	345.61	0.63
	5	339	338.97	1.28		11	345.7	345.75	0.71
	6	339.2	339.08	1.15		12	346.1	346.12	1.01
	7	339.4	339.36	2.50	1987	1	346.11	346.33	0.76
	8	340.0	340.00	1.23		2	346.06	346.07	0.69
	9	340	339.86	0.68		3	345.99	345.96	0.68
	10	339.8	339.61	0.59		4	345.97	346.04	1.19
	11	339.7	339.67	0.73		5	346.32	246.27	1.59
	12	339.7	339.68	0.83		6	346.72	346.52	1.74
1983	1	339.9	339.96	0.75		7	347.1	347.06	2.28
	2	340.3	340.32	1.04		8	347.42	347.41	3.62
	3	340.3	340.27	1.46		9	347.56	347.55	1.03
	4	340.6	340.58	0.98		10	347.7	347.8	0.91
	5	340.8	340.74	1.21		11	347.81	347.81	0.87
	6	341.2	340.95	2.04		12	348.45	348.43	0.98
	7	341.7	341.56	2.26	1988	1	349.15	349	0.98
	8	342	341.86	1.11		2	348.35	348.32	0.76
	9	341.9	341.94	1.46		3	348.16	348.2	1.05
	10	341.8	341.77	0.72		4	348.13	348.1	1.68
	11	341.8	341.77	0.89		5	348.19	348.23	2.16
	12	341.8	342.22	0.75		6	348.45	348.49	1.97
1984	1	341.9	341.82	0.69		7	349.28	349.08	2.14
	2	341.6	341.61	0.52		8	349.88	349.82	2.02
	3	341.7	341.82	0.56		9	349.26	349.38	1.61
	4	341.6	341.76	0.89		10	350.26	350.14	1.02
	5	341.6	341.53	1.57		11	349.97	349.87	1.25
	6	341.9	341.76	1.20		12	(349.89)		1.11
	7	342.4	342.22	1.41	1989	1	(349.83)		1.03
	8	343	342.98	1.45		2	349.76	349.75	0.66
	9	343.1	343.04	0.90		3	349.77	349.77	0.75
	10	342.8	342.8	0.69		4	349.8	349.86	1.02
						5	349.65	349.73	1.86

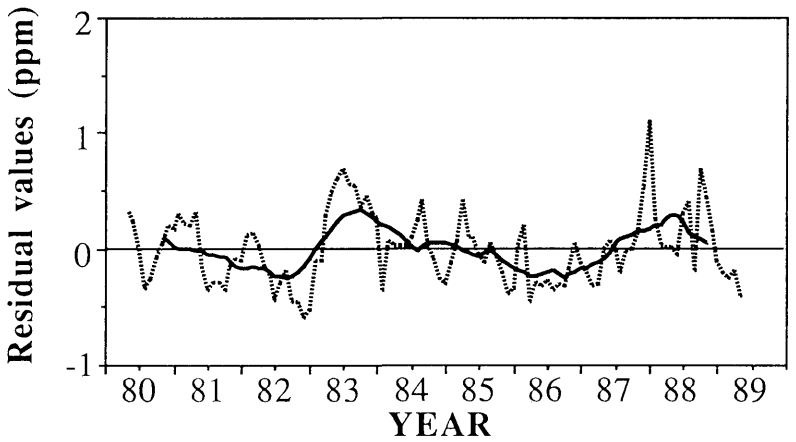

Fig. 2. Difference $r(t)$ between the observed monthly mean concentrations ($y(t)$) and the 4th degree polynomial P4(t) (dotted curve), and the corresponding smoothed spline (solid curve ($L(t)$) calculated by means of a 12-month running mean of $r(t)$.

yearly smoothed using a 12-month running mean, expressed in ppm year^{-1}. The same treatment is applied to the stations of Amsterdam Island, South Pole (Keeling et al., 1989), Cape Grim (Beardsmore and Pearman, 1987, 1989) and Mauna Loa (Keeling et al., 1989). Even though the intercalibration between different stations should be improved and additional effort concerning the selection of data should be made to validate such comparisons, these curves display a maximum in 1983, whose magnitudes of 2 ppm year^{-1} are very similar. The phases are quite the same at Amsterdam Island, Mauna Loa and South Pole, but seem to be earlier at Cape Grim. Conversely, in 1987–1988, a second maximum of these curves appears, with different magnitudes at South Pole, Mauna Loa and Amsterdam Island. A small difference of shape exists in 1985–1986 at Amsterdam Island, where we do not observe a slight decrease of the increase rate as shown in the other stations.

Table 2. *Coefficients of the 4th degree polynomials simulating the long-term evolution of the atmospheric CO_2 concentrations, P4(t) for all ^{222}Rn values (coefficients a_n) and Q4(t) for $^{222}Rn <$ 1 pCi m^{-3} (coefficients b_n)*

Degree n	a_n	b_n
0	336.89	336.93
1	$10.135 \cdot 10^{-2}$	$9.3937 \cdot 10^{-2}$
2	$-6.3935 \cdot 10^{-4}$	$-4.3489 \cdot 10^{-4}$
3	$1.2910 \cdot 10^{-5}$	$1.0874 \cdot 10^{-5}$
4	$-5.1217 \cdot 10^{-8}$	$-4.4477 \cdot 10^{-8}$

As mentioned above, the 12-month increase rates have been compared to the Southern Oscillation Index (SOI), which is an important parameter characterizing basic atmospheric changes, and, in the Pacific Ocean, is preceeding the installation of El Niño. Indeed, in Fig. 3, there is an obvious negative correlation between SOI and dCO_2/dt, as well at Amsterdam Island as at other background monitoring stations.

A phase lag appears between the minimum of SOI and the maximum of dCO_2/dt, determined at Amsterdam Island. This was also observed by Elliott and Angell (1987) in other stations and for ENSO events of 1972–73 and 1982–83. We calculated linear correlations between SOI and dCO_2/dt, for different phase lags in the dCO_2/dt data set. The correlation coefficients obtained just for the period of the 1982–83 and 1986–88 ENSO events are plotted in Fig. 4. The best regressions of about 0.9 were obtained with delays of 5 to 6 months, and 3 to 4 months, for the 1983 and 1987 events respectively. Therefore, the possible effect of the ENSO event was observed at Amsterdam Island, about 2 months earlier in 1987 than in 1983.

Furthermore, in Fig. 3, we also observe at all the stations: South Pole, Cape Grim, Amsterdam Island and Mauna Loa a hump in 1985, which is

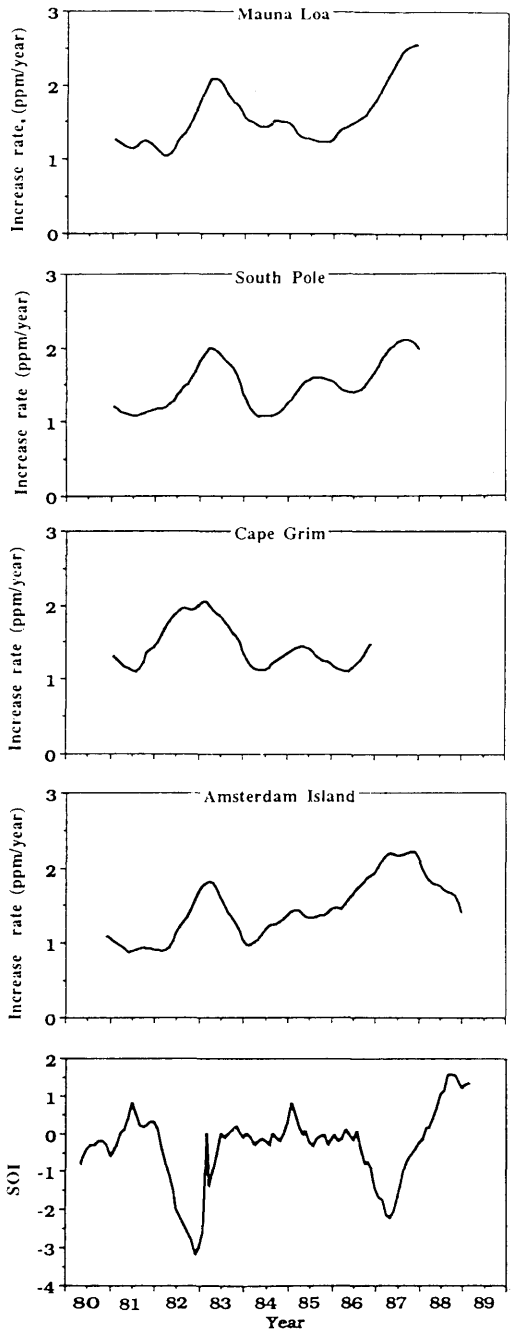

Fig. 3. Comparison between the atmospheric CO_2 increase rate, calculated according to the same mathematical treatment, at Mauna Loa, Amsterdam Island, Cape Grim (Tasmania) and the Southern Oscillation Index (SOI).

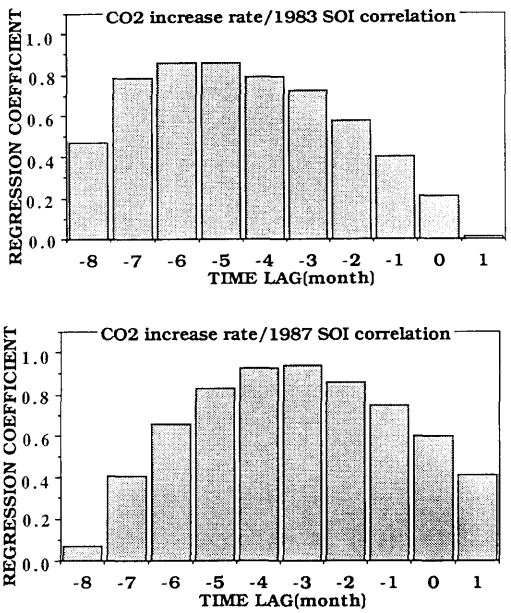

Fig. 4. Lag correlations between the CO_2 increase rate and SOI in 1983 (top) and 1987 (bottom).

not clearly correlated to the SOI. This effect is significantly smaller at Mauna Loa and Amsterdam Island, and appears progressively earlier when shifting northwards. It seems that differences in the atmospheric circulation at different latitudes could modulate the variation in CO_2 increase. It is possible to study this effect at Amsterdam Island, because ^{222}Rn has been continuously monitored there.

It has been shown by Polian et al. (1986) that Radon 222, a natural 3.8-day half-life radioactive noble gas, which is mainly injected into the atmosphere from the continental soils, is a good tracer of air masses advected from South Africa to Amsterdam Island. ^{222}Rn peaks are obtained in winter, when cyclonic systems sweep South Africa, and thus continental air is drawn southeastwards, between warm and cold fronts. The measurement technique, giving one value every two hours, was described in the same paper.

We selected ^{222}Rn data according the same criteria already mentioned defining typically marine air masses (i.e., $260° < \text{direction} < 300°$ and velocities $> 8\ m\ s^{-1}$ and $300° < \text{direction} < 360°$ and $0° < \text{direction} < 40°$ with velocities $> 4\ m\ s^{-1}$). This is important to discard eventual

emissions from the Island, when the air mass crosses the Island. By using this set of selected ^{222}Rn data, and applying the same 12-month running mean of monthly values as for CO_2, we obtain the curve in Fig. 5, compared with the SOI. The accuracy of each radon measurement is of the order of 20%. However, most of the errors being random, the monthly mean values are determined with an accuracy better than 5%. For the trend observed between 1980 and 1989, a possible shift due to the metrology of the order of 20% cannot be ruled out. As the observed shift is about 50%, it is significantly due to natural causes.

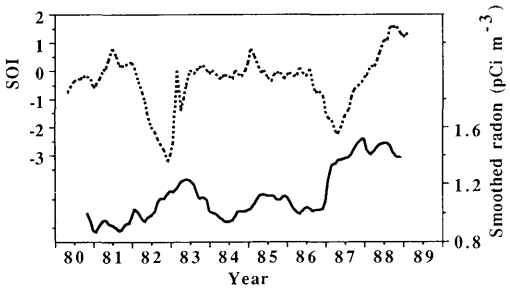

Fig. 5. Southern oscillation index (SOI: solid). Seasonally adjusted mean ^{222}Rn concentrations (pCi m^{-3}) at Amsterdam Island (Dashed).

In Fig. 5, a negative correlation seems also to appear between SOI and the seasonally adjusted ^{222}Rn. The same regression treatment for determining phase lags was performed between SOI and the seasonally adjusted Radon. Fig. 6 gives the results. The same delay of 6 months and a good correlation coefficient (close to 0.9) is found for the 1983 ENSO. In contrast, a very poor regression is obtained for the 1987 ENSO. Thus, the 1982–83 Southern Oscillation might have triggered also modifications of the atmospheric circulation in the Indian Ocean, increasing advection processes of continental air from Africa to Amsterdam island. This is much less clear for the 1987 Southern Oscillation.

In order to discard CO_2 variations ascribed to transport from South Africa, initial CO_2 data corresponding to the marine sector are selected a second time for ^{222}Rn concentrations (also by marine sector) smaller than 1 pCi m^{-3} of air, this threshold corresponding to the lack of recent continental influence. Subsequently, we applied the same mathematical treatment as before, with similar functions, i.e., a 4th degree polynomial, $Q4(t)$, whose coefficients are also expressed in Table 2, then $L'(t)$ and finally a derivative function of $Q4(t) + L'(t)$. The result is shown in Fig. 7, where both curves, relative to all data and to data with $Rn < 1$ pCi m^{-3}, are barely distinguishable. However, it can be seen in Fig. 7 that the CO_2

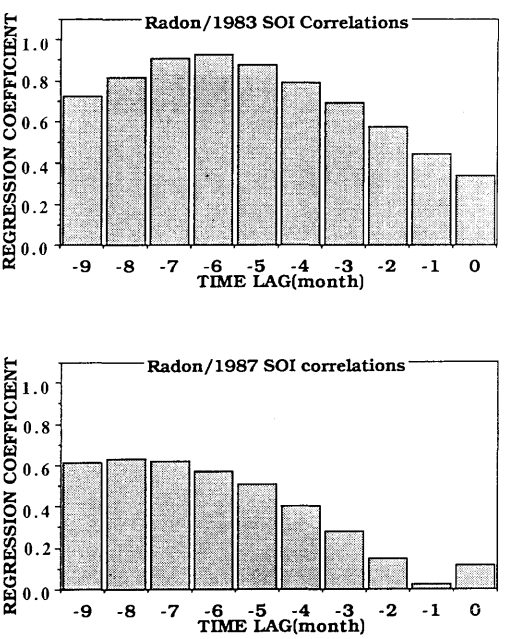

Fig. 6. Lag correlations between the seasonally adjusted ^{222}Rn and SOI in 1983 (top) and 1987 (bottom).

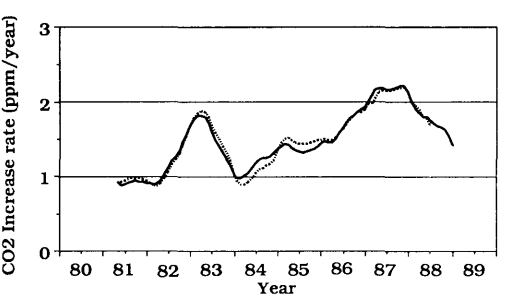

Fig. 7. Increase rate of the atmospheric CO_2 concentrations. The solid curve is obtained with all ^{222}Rn data. The dotted curve is obtained with data when $^{222}Rn <$ 1 pCi m^{-3}.

increase rate calculated for those latter data (excluding recent continental advections, i.e., $Rn < 1$ pCi m^{-3}) was smaller in 1984 and higher in 1985 than for the set of data with all Rn values, leading to the existence of a small hump, similar to those existing at South Pole and Cape Grim. Consequently, at Amsterdam Island this hump was likely smoothed by recent short-term continental CO_2 emissions from South Africa in 1984, and further by their reduction in 1985.

4. Discussion

This study confirms that global scale climatic events are able to modify significantly the increase rate of the atmospheric CO_2. This rate is positively correlated to the tropical SST, as shown by Elliott and Angell, (1987), and still much more clearly negatively correlated to the Southern Oscillation Index. The observed additional CO_2 increase due to this process is very close to 1 ppm per event in the low troposphere. If the total atmosphere is affected, this correspond to a net accumulation of 2.2×10^{15} g C, for each event. The effect of these events is delayed by 3 to 6 months. All the CO_2 monitoring stations are concerned, with slightly variable delays. Consequently, this effect cannot be accounted for by simple changes of the atmospheric transport of CO_2, not even by inter-hemispheric transfers.

It may be pointed out that severe climatical modifications were observed in many regions during the 1982–1983 and 1987–1988 ENSO. Important excess of precipitation occurred in regions usually dry, like the western part of South America (Peru), in 1983. This enables increasing CO_2 emissions from the soils. Conversely, severe droughts were also observed during the same periods in other areas of the world: Australia, Africa, East part of South America. For instance, a consequence was, in 1983–1984, smaller than normal vegetation indexes over Africa (Malingreau and Tucker, 1987). The comparison between CO_2 and ^{222}Rn data at Amsterdam Island confirms the general changes of the atmospheric circulation in the Indian Ocean, during ENSO periods. However, the influence of the climate changes in South Africa was not a direct injection of CO_2 into the subantarctic latitudinal band, since the CO_2 records obtained either for all ^{222}Rn values or for only $^{222}Rn < 1$ pCi m^{-3} are practically identical.

It is worth to note that generally droughts favour enhanced biomass burning. For instance, Cahoon et al. (1990), estimated from satellite observations that, in 1987, between 6 May and 3 June, a huge fire covered at least 1.1×10^6 hectares in China and 3×10^6 hectares in the Soviet Union. These observations enabled Levine et al. (1990) to estimate the atmospheric release of CO_2 to about 0.1×10^{15} g C, that could have enhanced the CO_2 increase rate, but is not large enough to account for the observed increase of the CO_2 increase rate.

By using atmospheric CO_2 data and its $^{13}C/^{12}C$ isotopic composition, both observed at Mauna Loa, Hawaii, and South Pole, and a box diffusion model, Keeling et al. (1989), showed that the biosphere released up to 5×10^{15} g of C during warm events, then reabsorbed during cold periods, while the ocean only withdrawed simultaneously much smaller amounts of the order of 1×10^{15} g C $year^{-1}$, per event. Thus, the main cause of CO_2 release to the atmosphere during ENSO periods, should be the continental biosphere, through important changes of precipitations over continents. Conspicuously, the biomass burning is included in this continental flux.

Another estimate was proposed by Tans et al. (1989) who used the GMCC data and an atmospheric transport model, to study sources and sinks of atmospheric CO_2. Focussing on the period of 1982–1983, they found, between 1982 and 1983, a disappearance of the southern ocean sink (-0.1×10^{15} g C $year^{-1}$ in 1983, instead of 1.2×10^{15} g C $year^{-1}$ in 1982) and an enhanced northern hemisphere source (between 17°N and 90°N), of 2.6×10^{15} g C emitted in 1983 instead of 1.4×10^{15} g C in 1982. This effect is possibly due to both a decreased ocean sink and a response of the land biosphere to the ENSO related perturbations.

Finally, even though the effects of ENSO events on the CO_2 flux are not yet well evaluated, it is clear that the CO_2 increase rate is significantly modified by large scale climatic events. This observation might account for the CO_2 increase, faster during the end of the 1980 decade than during the beginning, despite a relatively constant anthropogenic contribution between 1980 and 1986, about 5.2×10^{15} g of C $year^{-1}$ (Rotty, 1987; Marland, 1989), and a slow increase since 1986, due to the

recovery of the economical activity. This must be kept in mind when CO_2 scenarios are projected.

5. Acknowledgements

This work is supported by the subprogram/ CO_2/IGBP of the CNRS, the European Community Commission (Contract N° EV4/C1/ 00023), and the Territoire des Terres Australes et Antarctiques Françaises. We thank the staff in charge of the monitoring CO_2 and ^{222}Rn at Amsterdam island. We thank Dr. J. C. Duplessy and the two referees for their helpful discussions. This is the CFR contribution n° 1131.

REFERENCES

Ascensio-Parvy, J. M., Gaudry, A. and Lambert, G. 1984. Year-to-year CO_2 variations at Amsterdam Island in 1980–1983. *Geophys. Res. Lett. 11, 12,* 1215–1217.

Bacastow, R. B. 1979. Modulation of atmospheric carbon dioxide by the Southern Oscillation. *Nature 261,* 116–118.

Barnola, J.-M., Raynaud, D., Korotkevich, Y. S. and Lorius, C. 1987. Vostok ice core provides 160,000-year record of atmospheric CO_2. *Nature 329,* 408–414.

Beardsmore, D. J. and Pearman, G. I. 1987. Atmospheric carbon dioxide measurements in the Australian region: data from surface observatory. *Tellus 39B,* 42–66.

Beardsmore, D. J. and Pearman, G. I. 1989. Annual atmospheric CO_2 for 1986 and 1987 from Cape Grim, Tasmania. In: *World Meteorological Organization/ Technical Document* no. 306, 91–95, WMO Secretariat, Geneva, Switzerland.

Cahoon, D. R., Jr, Levine, J. S., Minnis, P., Tenille, G. M., Yip, T. W., Heck, P. W. and Stocks, B. J. 1990. The great Chinese fire of 1987: the view from space, *Chapman Conference on Global Biomass Burning,* Williamsburg, Virginia, USA, 19–23 March, 1990.

Elliott, W. P. and Angell, J. K. 1987. On the relationship between atmospheric CO_2 and equatorial sea-surface temperature. *Tellus 39B,* 171–183.

Gaudry, A., Ascensio, J. M. and Lambert, G. 1983. Preliminary study of CO_2 variations at Amsterdam Island (Territoire des Terres Australes et Antarctiques Françaises), *J. Geophys. Res. 88,* 1323–1329.

Gaudry, A., Monfray, P., Polian, G. and Lambert, G. 1987. The 1982–1983 El Niño: a 6 billion ton CO_2 release. *Tellus 39B,* 209–213.

Keeling, C. D., Bacastow, R. B., Carter, A. F., Piper, S. C., Whork, T. P., Heimann, M., Mook, W. G. and Roeloffzen, H. 1989. A three-Dimensional Model of Atmospheric CO_2 Transport Based on Observed Winds: 1-Observational Data and Preliminary Analysis. In "Aspects of Climate variability in the Pacific and western America" *AGU Geophysical Monograph* (ed. D. M. Peterson), Washington D.C, 165–363.

Komhyr, W. R., Gammon, R. H., Harris, T. B., Waterman, L. S., Conway, T. J., Taylor, W. R. and Thoning, K. W. 1985. Global atmospheric CO_2 distribution and variations from 1968–1982 NOAA/GMCC CO_2 flask-sampling data. *J. Geophys. Res. 90,* 5567–5596.

Levine, J. S., Cofer, W. R. III, Winstead, E. L., Hoffmann, K. G. and Stocks, B. J. 1990. The great Chinese Fire of 1987: Emission of Trace Gases to the atmosphere, *Chapman Conference on Global Biomass Burning.* Williamsburg, Virginia, USA, March 19–23.

Machta, L., Hanson, K. and Keeling, C. D. 1977. Atmospheric carbon dioxide and some interpretations. In: *The fate of fossil fuel CO_2 in the oceans* (eds. N. Anderson and A. Malahoff), Plenum Press, New York, 131–144.

Maligreau, J.-P. and Tucker, C. J. 1987. Vegetation observed from space. (La végétation vue de l'espace) *La Recherche 185,* 180–188.

Marland, G. 1989. Fossil fuels CO_2 emissions: three countries account for 50% in 1986. In: *Carbon dioxide information analysis center communications. Oak Ridge National Laboratory, Oak Ridge, TN,* 1–4.

Newell, R. E. and Weare, B. C. 1977. A relation between atmospheric carbon dioxide and Pacific sea surface temperatures. *Geophys. Res. Lett. 4,* 1–2.

Polian, G., Lambert, G., Ardouin, B. and Jégou, A. 1986. Long-range transport of continental radon in Subantarctic areas. *Tellus 38B,* 178–189.

Rotty, R. M. 1987. Estimates of seasonal variation in fossil fuel CO_2 Emissions. *Tellus 39B,* 184–202.

Tans, P. P., Conway, T. J., Nakazawa, T. 1989. Latitudinal distribution of the sources and sinks of atmospheric Carbon Dioxide derived from surface observations and atmospheric transport model. *J. Geophys. Res. 94, D4,* 5151–5172.